Great geomagnetic storm of 9 November 1991: Association with a disappearing solar filament

E. W. Cliver,[1] K. S. Balasubramaniam,[1] N. V. Nitta,[2] and X. Li[3]

Received 31 March 2008; revised 28 August 2008; accepted 13 November 2008; published 14 February 2009.

[1] We attribute the great geomagnetic storm on 8–10 November 1991 to a large-scale eruption that encompassed the disappearance of a ~25° solar filament in the southern solar hemisphere. The resultant soft X-ray arcade spanned ~90° of solar longitude. The rapid growth of an active region lying at one end of the X-ray arcade appears to have triggered the eruption. This is the largest geomagnetic storm yet associated with the eruption of a quiescent filament. The minimum hourly *Dst* value of −354 nT on 9 November 1991 compares with a minimum *Dst* value of −161 nT for the largest 27-day recurrent (coronal hole) storm observed from 1972 to 2005 and the minimum −559 nT value observed during the flare-associated storm of 14 March 1989, the greatest magnetic storm recorded during the space age. Overall, the November 1991 storm ranks 15th on a list of *Dst* storms from 1905 to 2004, surpassing in intensity such well-known storms as 14 July 1982 (−310 nT) and 15 July 2000 (−317 nT). We used the Cliver et al. and Gopalswamy et al. empirical models of coronal mass ejection propagation in the solar wind to provide consistency checks on the eruption/storm association.

Citation: Cliver, E. W., K. S. Balasubramaniam, N. V. Nitta, and X. Li (2009), Great geomagnetic storm of 9 November 1991: Association with a disappearing solar filament, *J. Geophys. Res.*, *114*, A00A20, doi:10.1029/2008JA013232.

1. Introduction

[2] Following *Newton* [1943], and prior to *Joselyn and McIntosh* [1981], solar flares were widely considered to be the sole source of great sporadic geomagnetic storms. During that time, however, *Dodson and Hedeman* [1964] wrote: "Even among the lists of exceedingly severe geomagnetic storms there are cases, albeit few in number, for which the evidence of flare-association is not convincing ... [with] no reports of major flares, short-wave fades, or major radio-frequency events within suitable preceding time intervals. It is possible that [such] storms constitute a warning that the cause of severe geomagnetic storms, even of the apparently sporadic type or with SCs [sudden commencements], may not always rest with the seemingly suitable precedent flares that we currently associate with them."

[3] Today we recognize the cautionary statement of *Dodson and Hedeman* [1964] as a precursor of the general recognition, which came nearly 30 years later, that certain CMEs, rather than the major flares with which they were characteristically, but not always, associated, were the essential element for producing great sporadic storms [*Kahler*, 1992; *Gosling*, 1993]. The reviews of Kahler and Gosling built in part on the analysis of *Joselyn and McIntosh* [1981], who associated the major geomagnetic storm of 27–28 August 1978 with the disappearance of a large quiescent solar filament on 23 August. Subsequently, *Cliver and Crooker* [1993] associated a great "problem" storm on 28 October 1961 (to which *Dodson and Hedeman* [1964] initially drew attention) with a disappearing solar filament (DSF) (lying, by definition [see, e.g., *Bruzek and Durrant*, 1977, sections 9.10 and 10.7], outside an active region) on 25 October of that year and *McAllister et al.* [1996] associated a great storm on 17 April 1994 with the formation of an extended (~150° east-west and 30–40° north-south) high-latitude soft X-ray arcade, a signature of a major solar eruption, on 14 April. The 17 April event represents an extreme example of a problem storm in that the long segment of chromospheric neutral line over which the eruption occurred was marked only by filament channels (FC) [*Martin*, 1998] and small and faint filaments. A fourth example of a major *Dst* storm with a quiet Sun source (i.e., lying outside of both active regions and coronal holes) was recently reported by *Zhang et al.* [2007], who determined the solar sources of all large ($Dst \leq -100$ nT) geomagnetic storms during solar cycle 23 (1996–2005). They linked a storm on 22 October 1999 with a DSF-associated eruption originating outside an active region late on 17 October.

[4] *Joselyn and McIntosh* [1981] subdivided geomagnetic storms according to their solar sources: flares, disappearing solar filaments (DSFs or eruptions of the magnetic field overlying FCs) outside of active regions, and coronal holes. Today we combine the first two of these sources under coronal mass ejections (CMEs). The earlier distinction is worth keeping in mind for a practical reason: the difficulty in forecasting storms that originate in solar eruptions outside

[1]Space Vehicles Directorate, Air Force Research Laboratory, Hanscom Air Force Base, Massachusetts, USA.
[2]Lockheed Martin Solar and Astrophysics Laboratory, Palo Alto, California, USA.
[3]Laboratory for Atmospheric and Space Physics, Boulder, Colorado, USA.

0148-0227/09/2008JA013232

Table 1. The 25 Largest Geomagnetic Storms Based on the *Dst* Index, 1905–2004[a]

Date	Time (UT h)[b]	Peak Value	References[c]
25 Sep 1909	17	−670	1
28 Mar 1946	14	−569	4
14 Mar 1989	1	−559	5
5 Jul 1941	13	−484	2
20 Nov 2003	19	−457	7
1 Mar 1941	18	−428	3
8 Jul 1928	8	−423	4
13 Sep 1957	10	−420	5
15 Jul 1959	19	−415	5
11 Feb 1958	11	−412	5
23 Mar 1923	3	−409	4
30 Oct 2003	22	−385	7
19 Sep 1941	6	−384	1
26 May 1967	4	−382	5
9 Nov 1991	1	−354	6
30 Apr 1960	18	−353	5
22 Jan 1938	11	−349	1
8 Jul 1958	20	−348	5
25 Jan 1938	23	−348	4
31 Mar 2001	8	−347	7
8 Nov 2004	6	−347	7
24 Mar 1940	20	−339	2
1 Apr 1960	18	−338	5
13 Nov 1960	9	−336	5
11 Aug 1919	10	−328	4

[a]Based on *Love*'s [2007] extension of the *Dst* index (J. J. Love, personal communication, 2008). The great storm of May 1921 which may, in fact, be the largest storm of the last ~100 years [*Kappenman*, 2006], ranks 26th on the list and is currently being reevaluated using additional data. At most stations the magnetometers were driven off-scale for this event.

[b]The time refers to the minimum hourly value of *Dst*.

[c]References: 1, *Newton* [1943]; 2, *Newton* [1944]; 3, *Newton* [1948]; 4, *Jones* [1955]; 5, *Cliver and Crooker* [1993]; 6, 1991 Boulder Preliminary Report of Solar-Geophysical Data (BPR/SGD); 7, *Zhang et al.* [2007].

of active regions and thus lack strong flare emissions. Given this difficulty, it is useful to consider the limiting size of such storms in comparison with those with other types of solar sources. The largest flare-associated *Dst* storm since 1905 (based on a recent extension of the *Dst* index [*Love*, 2007; J. J. Love, personal communication, 2008] that will be used throughout this paper) was the great storm of 25 September 1909 [*Lockyer*, 1909; *Hale*, 1931; *Silverman*, 1995] which had a minimum hourly *Dst* value = −670 nT. The largest such storm during the space age was the well-known space weather event of March 1989 [*Allen et al.*, 1989] which had a minimum hourly *Dst* value of −559 nT. The largest 27-day recurrent storm (attributed to a high-speed stream/co-rotating interaction region [*Crooker and Cliver*, 1994]; see also *Krieger et al.* [1973], *Gulbrandsen* [1973], and *Neupert and Pizzo* [1974]) from 1972 to 2005 had a minimum *Dst* value of −161 nT [*Richardson et al.*, 2006; *Zhang et al.*, 2007]. The minimum *Dst* values of the four storms discussed above that originated in quiet Sun regions were as follows: 28 October 1961, −267 nT; 28 August 1978, −216 nT; 17 April 1994, −189 nT; and 22 October 1989, −232 nT. Two other storms without strong solar associations mentioned by *Dodson and Hedeman* [1964], 4 September 1958 (−289 nT; this event was preceded by a 1+ flare at E84) and 5–7 October 1960 (−236 nT), may also have originated in quiet Sun regions [*Cliver and Crooker*, 1993].

[5] In this paper, we document a storm that originated in an eruption outside of an active region that surpassed all six of these (real or putative) quiet Sun events. During the great storm of 9 November 1991, the minimum hourly *Dst* reached −354 nT. Our analysis is presented in section 2 and results are summarized and discussed in section 3.

2. Analysis

2.1. A Search for Major Magnetic Storms From Quiet Sun Regions, 1905–2004

[6] Table 1, compiled from Love's extension of the *Dst* index back to 1905, lists the 25 largest *Dst* storms recorded from 1905 to 2004 [cf. *Cliver and Svalgaard*, 2004]. None of the six large problem storms mentioned in section 1 appears on this list of events, each being too small.

[7] To determine if Table 1 contained any storms originating outside of active regions, we relied on the work of *Newton* [1943, 1944, 1948], *Jones* [1955], *Cliver and Crooker* [1993], the 1991 Boulder Preliminary Report of Solar-Geophysical Data (BPR/SGD), and *Zhang et al.* [2007] for solar source identifications. From these references we obtained sources (either suitable flares or, for times when flare observations were unavailable, large/favorably located active regions) for all but one of the listed storms. (For the storm on 25 January 1938, *Jones* [1955] suggests a flare "33 hours earlier at the extreme position of 82° west of the Sun's central meridian over Group 12673" (mean area during disk passage = 2955 millionths of a hemisphere).)

[8] Only the great storm from 8 to 10 November 1991 lacked association with a major solar flare (or strong candidate active region). This storm began with a sudden commencement at 0648 UT on 8 November and reached its minimum hourly *Dst* value of −354 nT at 01 UT on 9 November (Figure 1). Quoting from the BPR/SGD for that year, as written by the Space Weather Prediction Center forecasters: "The most likely source of this disturbance is thought to be the disappearance of the 24 degree long filament from the southeast quadrant on 6 [meaning between 5–6] November." It is noteworthy that no advance warning was issued for this major storm, which ranked 15th in size

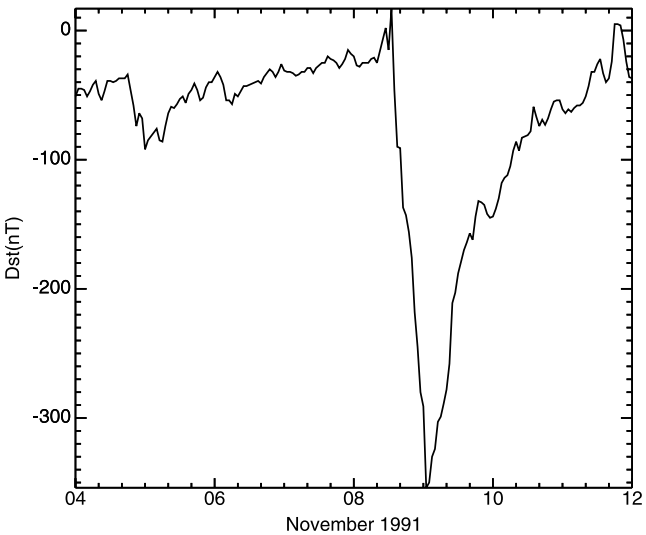

Figure 1. *Dst* geomagnetic index, 4–11 November 1991.

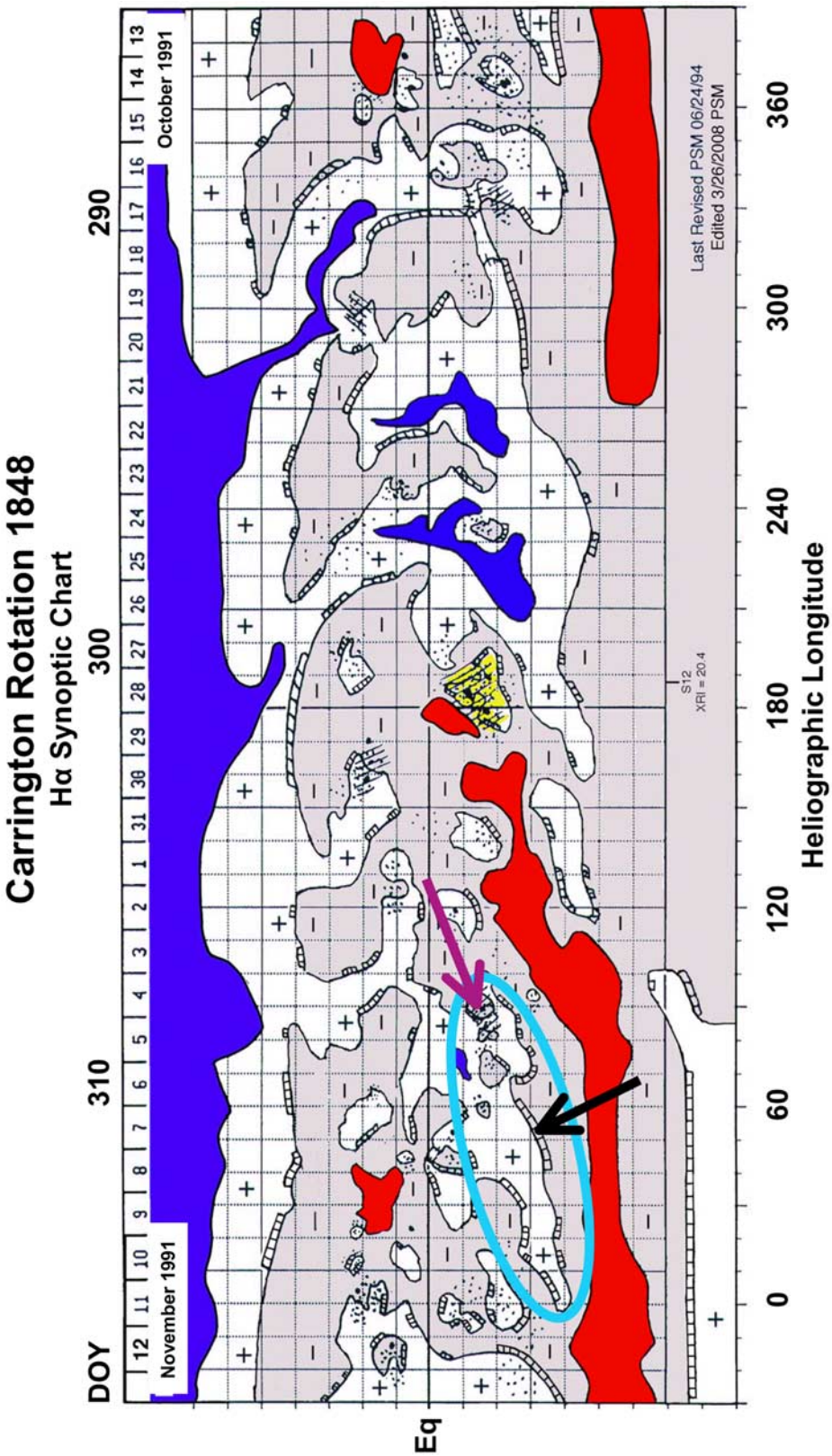

Figure 2. Hα synoptic plot of Carrington Rotation 1848 in October–November 1991. The light blue oval indicates the section of large-scale chromospheric neutral line that erupted to give rise to the great *Dst* storm of 8–10 November 1991. The black arrow points to the quiescent filament that disappeared, and the magenta arrow points to AR 6906, the site of newly emerging flux in early November. Active Region 6891, highlighted in yellow, was a prolific producer of M-class and X-class flares with an X-ray Region Index (XRI) ≥ 10 [*McIntosh*, 1990, 1993]; it was $\sim 20^{\circ}$ behind the west limb at the time of the eruption responsible for the great storm.

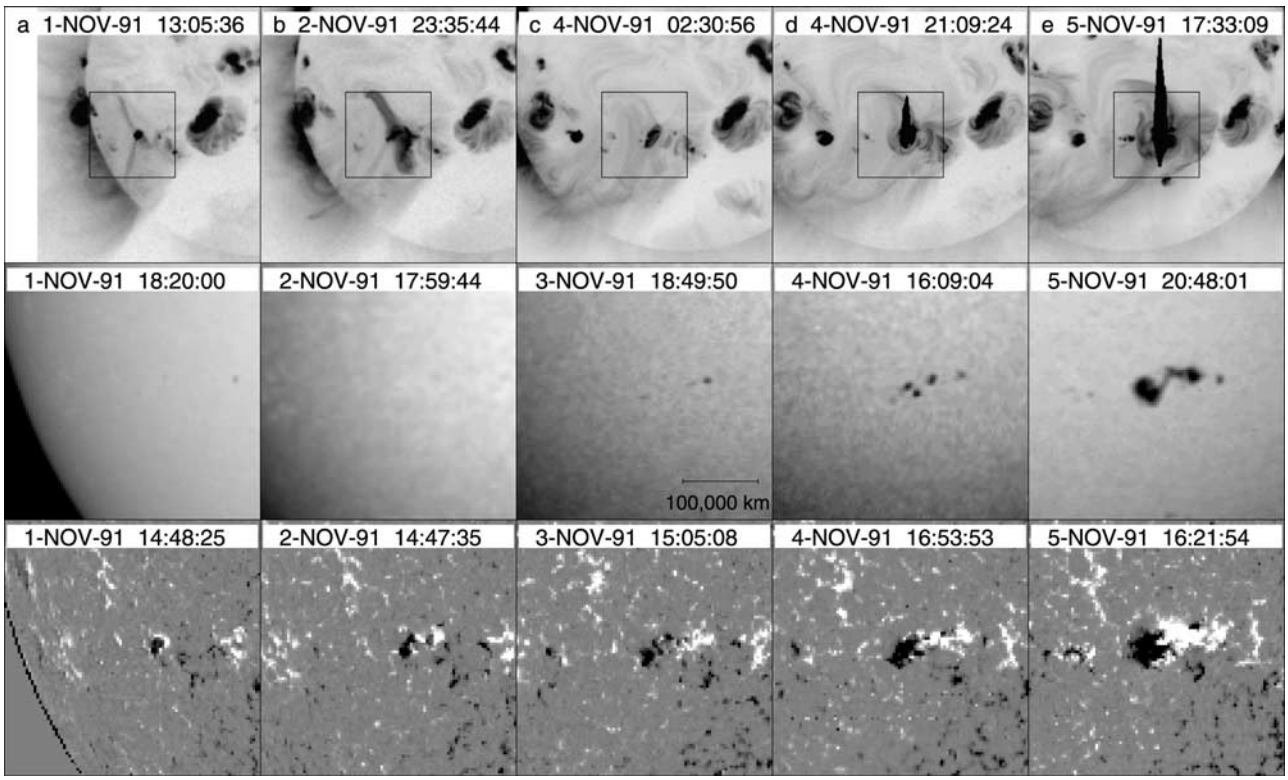

Figure 3. Sequences of images from (top) *Yohkoh* SXT (reverse color), (middle) the *Yohkoh* white-light telescope, and (bottom) the Kitt Peak magnetograph (white, positive polarity; black, negative polarity) for 1–5 November. The boxes in the top panel are centered on NOAA AR 6906, which rapidly evolved between 3 and 5 November. The vertical artifacts in AR 6906 on 4 and 5 November in SXT data are due to small C-class flares. In these and subsequent solar images, solar north is to the top, and west to the right.

(as measured by *Dst*) of magnetic storms between 1905 and 2004, surpassing such well-known events as the July 1982 event for which the responsible interplanetary disturbance produced detectable radio emission from the termination shock of the heliosphere [*Gurnett et al.*, 1993] and the storm linked to a major solar eruption on "Bastille Day" 2000 [*Watari et al.*, 2001]. The November 1991 storm was the largest event from March 1989 until late in the present cycle, when it was exceeded in intensity by two flare-associated events: 30 October 2003 (−384 nT) and 20 November 2003 (−457 nT) [*Gopalswamy et al.*, 2005a, 2005b; *Zhang et al.*, 2007].

2.2. Solar Observations of the Source of the November 1991 Storm

2.2.1. Global Context

[9] Figure 2 gives the Hα synoptic chart from 13 October to 12 November 1991, encompassing Carrington Rotation (CR) 1848. The key element of Hα synoptic charts [*McIntosh*, 1979; *Fox et al.*, 1998; *McIntosh*, 2003] is the delineation of large-scale chromospheric neutral lines, via filaments and filament channels, and, when these tracers are not present, inferred interconnections based on continuity and guided by coronal hole (from He 10830 Å observations) and active region locations. The eruption responsible for the November 1991 storm occurred over the neutral line segment (from ∼0–100° heliolongitude) lying inside the light blue oval; a black arrow marks the filament that erupted.

[10] Figure 3 contains sequences of images from the *Yohkoh* soft X-ray telescope (SXT; top), the *Yohkoh* white-light telescope (middle), and the Kitt Peak magnetograph (bottom) for 1–5 November. NOAA active region (AR) 6906, located at the top right of the light blue oval in Figure 2 and marked by the magenta arrow, is at the center of the boxes in the top panel. The white light images in the middle panel and the magnetograms in the bottom panel reveal the rapid growth in sunspot area of this region, from ∼20 millionths of a hemisphere late on 3 November to ∼80 millionths late on 4 November to ∼400 millionths late on 5 November, when the DSF-associated eruption occurred. Field lines extending from this region along the neutral line (indicated in Figure 2) to the southeast and northeast are apparent in the SXT images as early as 1 November and are well defined by 4 November. The rapid growth of AR 6906, and the magnetic loops extending from it toward the large filament to the southeast, suggest that the active region evolution destabilized the magnetic field overlying the large-scale neutral line.

2.2.2. Soft X-Ray and Hα Images

[11] To obtain an independent (from the Boulder forecasters) assessment of the source of the 9 November 1991 geomagnetic storm, we examined the GOES whole Sun soft X-ray curve from 4 to 7 November (Figure 4) as well as Hα images from the Sacramento Peak and Meudon Observatories (Figure 5) and *Yohkoh* SXT images (Figure 6). The candidate source events from SXT observations during this

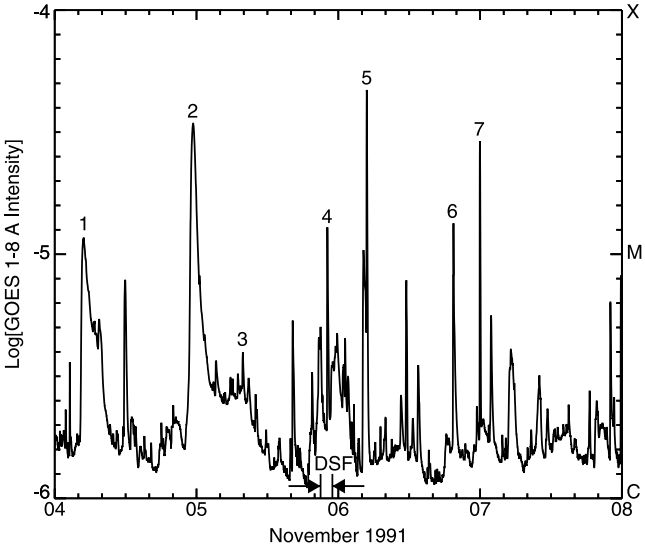

Figure 4. The 1–8 Å whole Sun soft X-ray intensity, 4–7 November 1991. Numbered soft X-ray flares are discussed in the text, and the timing of the DSF is indicated.

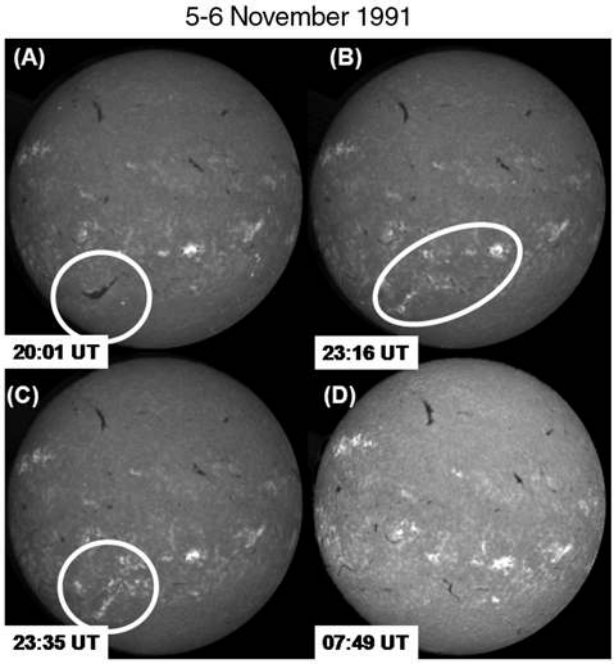

Figure 5. Hα images encompassing the times of the DSF-associated eruption on 5–6 November 1991. Figures 5a and 5b show "before" and "after" images of the DSF, with the filament circled in Figure 5a and the section of the large-scale neutral line which erupted encompassed by the oval in Figure 5b. In Figure 5c the two-ribbon brightening outlining the footprints of the erupted filament is circled. Figure 5d was taken during the secondary brightening of the soft X-ray arcade. Figures 5a–5c are from Sacramento Peak Observatory, and Figure 5d is from Meudon Observatory.

four day interval are listed in Table 2. The two long-duration M-class flares on 4 November are the most promising *prima facie* candidates in Figure 4 (events 1 and 2) but reference to Table 2 shows that both arose in AR 6891 (or adjacent AR 6892), then at the southwest limb, and are therefore unlikely sources of the great storm. The blended activity between 04 and 08 UT on 5 November (event 3) also arose in activity at the west limb. Only one of the events in Table 2 appears to have been capable of giving rise to the great storm on 8–10 November: the disappearance of a ~25°-long high-latitude filament (~S35E25) at ~23 UT on 5 November that was accompanied by an extended (~90°) soft X-ray arcade (and ~25°-long flare-like ribbons) in the southern hemisphere. In the series of Hα images in Figure 5, Figures 5a and 5b are "before" (with the filament circled) and "after" (with the extended section of the neutral line which erupted encompassed by the oval) images bracketing the disappearance of the filament. In Figure 5c, the faint two-ribbon brightening (circled) surrounding the former position of the filament (Figure 5a) was not reported as a flare in *Solar-Geophysical Data*. *Kiepenheuer* [1964] presciently viewed such DSF-associated brightenings as "soft" versions of active region flares. The faint brightenings in Figure 5c lie near one end of a continuum of eruptive events with prominent two-ribbon flares from active regions on the other end; both types of events are encompassed by the standard CSHKP picture [see, e.g., *Hudson and Cliver*, 2001] of solar eruptions. Figure 5d shows the Sun at ~ 08 UT on 6 November during the development of the large-scale soft X-ray arcade. In Figure 5d the upper part of the filament that disappeared late on November 5 has reformed and is more prominent than it was before the disappearance of the main section of the filament to the southeast.

[12] In the series of reverse-color SXT images in Figure 6, Figure 6a taken on 5 November at 2001 UT represents the

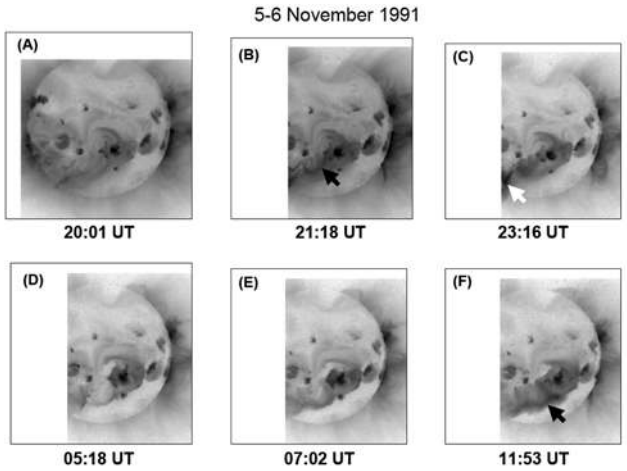

Figure 6. *Yohkoh* reverse color SXT images of the southern hemisphere streamer belt on 5–6 November 1991. The black arrow in Figure 6b indicates the loops which were enhanced following a C5 flare with maximum at 2059 UT in AR 6906. The white arrow in Figure 6c indicates intense brightening associated with the DSF, and the black arrow in Figure 6f points to the soft X-ray arcade near its maximum phase of development.

Table 2. Eruptive Signatures Seen in SXT Images During 4–7 November 1991

Date	Time	Location	Description
4 Nov	422	W limb	flare and loop expansion in AR 6891
4 Nov	1233	S15E10	two-sided jet in AR 6906, repeated at 1732
4 Nov	~2300	SW limb	eruption from AR 6891 preceded by loop expansion in the rising phase of a M3 flare
5 Nov	514	NW limb	eruptive flare in AR 6893
5 Nov	754	SW limb	small eruption in a quiescent region
5 Nov	1910	SE Quad	start of eruption of high-latitude filament
5 Nov	2045	SW limb	jet-like ejection from AR 6891
5 Nov	2316	S Hemi	DSF + ~90° arcade
5 Nov	2316	SW limb	expanding loops, repeated at 2110 on Nov. 6
7 Nov	721	SE limb	appearance of arcade
7 Nov	1716	SW limb	far-side eruption

pre-eruption state, with the pre-existing coronal helmet-streamer configuration visible but relatively faint. Figure 6b at 2118 UT shows loops (indicated by a black arrow) reaching from AR 6906 to the northern vicinity of the large filament; these loops had brightened following a C5 flare (Figure 4) with maximum at 2059 UT in AR 6906. In Hα, the filament began to erupt at ~2100 UT and disappeared by 2316 UT (Figure 5b). In SXT images, the associated coronal brightening is apparent as the dark feature (indicated by a white arrow) toward the bottom left of the frame taken at that time (Figure 6c). (In Figures 6b–6f, part of the Sun's western hemisphere is cut off as the SXT field of view was adjusted to focus on coronal activity from major AR 6891 (shaded yellow in Figure 2), then ~20° beyond the southwest limb of the Sun.) Note that by 0518 UT on 6 November (Figure 6d), the extended soft X-ray arcade has faded significantly but by 0702 UT (Figure 6e) it has clearly begun to brighten. This could indicate either delayed growth of the post flare loop system associated with the DSF-associated eruption late on the 5th (in which case the earlier brightening would correspond to the eruption itself) or a secondary eruption encompassing the same section of chromospheric neutral line. Given the cadence of SXT images (5 November–2316 UT; 6 November–0153 UT, 0223 UT, 0518 UT, 0548 UT, 0646 UT, 0702 UT, 1036 UT, 1136 UT, 1153 UT ...), we cannot be more definitive. That said, there seems no question that this eruption, either simple or complex, was the source of the great storm. Maximum brightness of the arcade is reached at ~1200 UT (Figure 6f).

[13] During the course of the DSF, at 2208 UT, an M1 flare, superimposed on a complex long duration ~C4 event, occurred in AR 6096 (event 4 in Figure 4). While this impulsive flare may have helped to further destabilize the filament (which began to erupt at ~2100 UT), it is not considered to be a candidate source for the great storm. Similarly the three M-class events on 6 November (events 5, 6, and 7) all from AR 6906, lack the long-durations of flares characteristically associated with great geomagnetic storms.

2.3. Solar Wind Observations

[14] In order to confidently link solar eruptions to geomagnetic storms, it is necessary to use solar wind speed data as a consistency check, applying empirical tools such as that developed by *Cliver et al.* [1990] and *Gopalswamy et al.* [2001] to make certain that measured solar wind speeds at Earth are compatible with shock transit times and CME speeds (where available) for a given solar source. Solar wind data for the November 1991 storm have a gap for much of 8 November, as can be seen in Figure 8, where the data points surrounded by blue diamonds (for magnetic field strength, B) and red circles (for speed, V) represent the available OMNI data and the uncloaked points represent assumed data, as discussed below. Fortunately, solar wind magnetic field data exist for the crucial period covering the peak of the storm as measured by the geomagnetic *Dst* (Figure 1) and *am* indices. The measured minimum hourly average B_Z value of −26.7 nT at 23 UT on 8 November corresponded to a total B magnitude of 30.8 nT. *Siscoe et al.* [1978] calculated that southward B_Z fields this strong occur on average about once per year.

2.3.1. Solar Wind Reconstruction From Geomagnetic Data

[15] High-confidence relationships have been developed over the years between geomagnetic data (which do not suffer from gaps) and solar wind parameters [*Svalgaard*, 1977; *Temerin and Li*, 2002]. Geomagnetic activity is driven primarily by the solar wind B and V. Because the widely used *am* and *Dst* geomagnetic indices [*Mayaud*, 1980] have different dependencies on these parameters, we can use them to fill data gaps in the following manner: (1) on the basis of experience and intuition, assume solar wind speed and magnetic field data for periods of missing data; (2) use these composite profiles (consisting of actual and assumed values) to derive one of the indices (in our case *am*, via *Svalgaard* [1977]); (3) adjust the assumed, gap-filling, solar wind parameters as necessary until the observed *am* is faithfully reproduced by the model; (4) use the various continuous solar wind parameter series obtained by this method (i.e., V, B_X, B_Y, B_Z, and n (density); with V and B_Z shown in Figure 7) to calculate the other index (*Dst*, via *Temerin and Li* [2002]) as a test of the method. For the November 1991 storm, this approach is validated by the reasonable agreement seen in Figure 8 between *Dst*

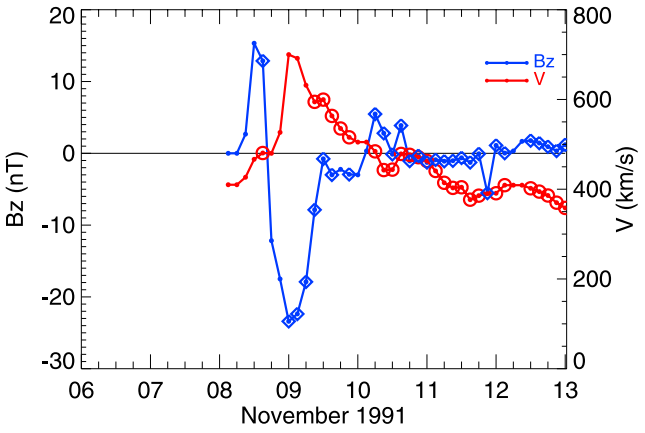

Figure 7. Solar wind V and B_Z data (3-h averages) for 8–10 November 1991. Data points surrounded by red circles (for V) or blue diamonds (for B_Z) were taken from the OMNI tape. Uncloaked points represent solar wind parameter values inferred from geomagnetic indices via an iterative process (section 2.3.1).

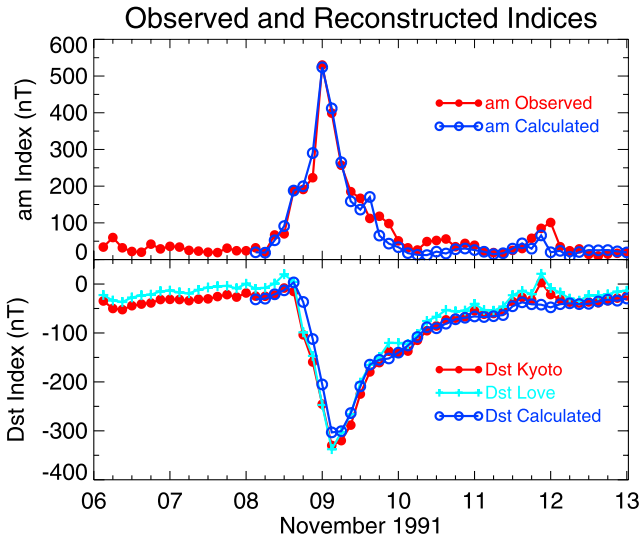

Figure 8. (top) Comparison of the actual *am* index with an *am* index constructed (via the *Svalgaard* [1977] model) from solar wind data for which gaps were filled by trial and error to reproduce the observed *am* index. (bottom) Comparison of the Kyoto (observed, 3-h averages) *Dst* index with the *Dst* index constructed by J. Love and a *Dst* index constructed (via the *Temerin and Li* [2002] model) using solar wind data for which gaps were filled with inferred values to reproduce the *am* index.

values derived from the composite (real and inferred) time series of solar wind parameters and *Dst* values determined from magnetometer observations. A variation of this method has also been employed to model the solar wind for the 1–2 September 1859 super storm [*Li et al.*, 2006].

2.3.2. Linking the Eruption to the Storm

[16] The peak solar wind speed obtained using the above approach was 725 km s^{-1} late on 8 November (Figure 7). Taking the time of the DSF to be ~2300 UT on the 5th, gives a Sun-Earth transit time of ~56 h for the interplanetary shock (sudden commencement at 0647 UT on 8 November) and an average transit speed of ~740 km s^{-1}. A point with coordinates of (740 km s^{-1}, 725 km s^{-1}) falls at the outer edge of the scatter in Figure 9 (taken from *Cliver et al.* [1990]). The location of the point for the November 1991 storm in this plot may be a reflection of its origin outside of an active region, in contrast to the large flare-associated events on which Figure 9 was based. We note that the two large "quiet Sun" storms discussed in the introduction for which solar wind data are available also lie above the general scatter (28 August 1978 (425 km s^{-1}, 480 km s^{-1}); 22 October 1999 (560 km s^{-1}, 515 km s^{-1})). (The data point with coordinates (940 km s^{-1}, 870 km s^{-1}) in Figure 9 was associated with a long duration M4 flare on 4 September 1982 of which the Boulder forecasters wrote in the BPR/SGD, "The M4 event was a parallel ribbon flare extending 20° along the large filament to the west of Region 3886.") Alternatively, or additionally, the November 1991 storm may have originated in a secondary eruption on 6 November (section 2.2.2), in which case the data point for this event would shift to the right and closer to the least squares line.

[17] An empirical shock arrival (ESA) model developed by Gopalswamy and colleagues relates T, the time in hours from CME onset at the Sun to shock arrival at 1 AU, to V, the average CME speed near the Sun, as follows:

$$T = a\left(b^{V}\right) + c, \text{where } a = 151.002, b = 0.998625, \text{and } c = 11.5981 \quad (1)$$

For the 5 November DSF-associated eruption, a T-range of 48–56 h yields a range in CME speeds from 890 to 1035 km s^{-1}. *Gopalswamy et al.* [2005b] used equation (1) to obtain the speeds of 22 historical (i.e., pre-coronagraph) CMEs, including six corresponding to great storms in our Table 1. The median CME speed for these six storms was ~1850 km s^{-1}, well above the maximum possible speed for the 5 November 1991 eruption. This is consistent with the well-established fact that CMEs from quiet Sun regions tend to have lower speeds than those originating in active regions [e.g., *Gosling et al.*, 1976].

3. Conclusion

3.1. Summary

[18] We associate the great storm of 8–10 November 1991 (*Dst* = −354 nT) with an eruption overlying an extended section of chromospheric neutral line outside of an active region. This is the largest storm yet documented that was associated with the eruption of a quiescent filament, exceeding that of 28 October 1961 (−267 nT [*Cliver and Crooker*, 1993]) by ~100 nT. For comparison, the largest coronal-hole-associated storms (at least during cycle 23) have minimum hourly *Dst* values ~−130 nT [*Zhang et al.*, 2007] while the largest flare-associated storm since 1905 had a minimum *Dst* value of −670 nT. Over all, the November 1991 storm was the 15th largest *Dst* event of the last 100 years. The solar signatures of the eruption responsible for the November 1991 storm include the

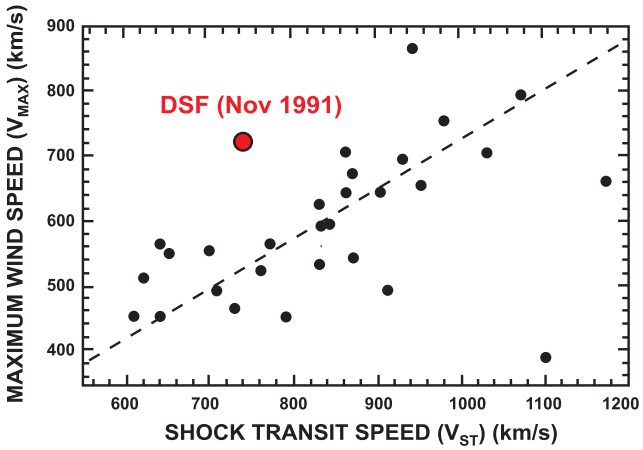

Figure 9. A plot of peak solar wind speed following an interplanetary shock at Earth versus the average shock speed from the Sun to the Earth for a sample of events observed from 1978–1982 [*Cliver et al.*, 1990]. The data pair for the November 1991 storm and its DSF solar source is indicated.

disappearance of a ~25° solar filament late on 5 November and the formation of a soft X-ray arcade spanning ~90° of longitude. The destabilization of the large-scale neutral line manifested by the eruption followed the rapid growth of NOAA AR 6096 which was located at one end of the transient soft X-ray arcade. We used empirical relationships between shock transit time, peak solar wind speed (deduced from geomagnetic indices for this event), and CME speed to substantiate the eruption/storm association.

3.2. Quiet Sun Sources of Great Storms

[19] The location of AR 6096 near the northwest end of the extended soft X-ray arcade indicates that the eruption on 5 November did not arise from a "pure" quiet Sun source. That said, the notion that emerging flux in an active region could destabilize a distant quiescent filament was arrived at long before instruments such as *Yohkoh* revealed magnetic connections between widely separated solar regions. *Bruzek* [1952] wrote, "...filament ascensions [associated with flare-like brightening outside an active region] are often caused by a disturbance which comes from a newly formed sunspot group...," precisely what appears to have happened in this case. Bruzek's pioneering study was recently updated and extended by *Feynman and Martin* [1995], who presented statistical evidence that "eruptions of quiescent filaments and associated coronal mass ejections ... occur as a consequence of the destabilization of large-scale coronal arcades due to interactions between these structures and new and growing active regions" (see Figure 6b for the 5 November 1991 DSF). It seems clear that AR 6096 and the impulsive flares it produced would not by themselves be considered promising candidates for association with a great geomagnetic storm. The outstanding solar event (near central meridian) during the time preceding the storm was the DSF and formation of the extended soft X-ray arcade, which lay largely outside AR 6096. In this sense, it is useful to retain the concept of quiet Sun sources of great geomagnetic storms.

[20] *Feynman and Ruzmaikin* [2004] documented a high-speed CME on 12 September 2000 that was associated with an erupting quiescent prominence and argued that such events serve to bridge the gap between the more common slow CMEs associated with DSFs and energetic CMEs that originate in active regions. While we inferred a relatively high CME speed of ~1000 km s^{-1} [after *Gopalswamy et al.*, 2005b] for the 5 November 1991DSF-associated eruption, this value is only about half the ~1800 km s^{-1} observed for the September 2000 event. There is a general similarity in the evolution of the 12 September and 5 November 1991 eruptions; in both cases newly emerging flux in the vicinity of a quiescent filament leads to slow destabilization of the filament followed by a strong acceleration phase and filament disappearance.

3.3. Predictability of Storms From Quiet Sun Eruptions

[21] It bears repeating that the first tier geomagnetic storm of November 1991, which was larger than any storm in the preceding cycle 21 (1976–1986) and was surpassed only by the great March 1989 event in solar cycle 22, went unpredicted. This missed forecast stemmed in part from the unavailability of real-time coronagraph and soft X-ray images to space weather forecasters in 1991, a situation which has since been rectified.

[22] Even with such observations available, however, the question arises: How predictable are storms with quiet Sun (DSF or FC) origins such as that in November 1991? *Joselyn* [1995] investigated the magnetic orientation of 46 major (≥20°, normal or dark) filaments that disappeared while near solar central meridian in 1979 and found mixed results. She found that no storms (with Ap ≥ 30) were associated with the least favorable orientation (negative fields north of an east-west filament; 0 of 7 cases), but few storms could be associated with the more favorable orientations (5of 15). Joselyn concluded from this limited but practical test that simple extrapolations using the observed filament orientation do not provide definitive predictions of field directions or storm occurrence at 1 AU. Similarly, *Webb* [1999], from a superposed epoch analysis of a sample of large (>20 square degrees), dark, central meridian (midpoints < 30° from central meridian) DSFs (taken from the 1964–1980 catalog compiled by *Wright* [1991]), found no statistically significant effect on geomagnetic activity (either *Dst* or *ap*), substantiating an earlier result by *Wright* [1991]. Finally, we note that while the filament that disappeared on 5 November 1991 was large (~25°) and well positioned (~S35E25) with an inferred favorable leading edge polarity (southward), the filament alignment in relation to Earth's dipole axis was more nearly north-south than east-west. In this regard, the source of the 8–10 November 1991 storm may have been similar to that for the great storm of 20 November 2003 [*Gopalswamy et al.*, 2005a]. Those authors attributed the largest storm of cycle 23 to the axial component of a magnetic cloud that was highly inclined to the ecliptic plane. These various results indicate that forecasts of storms originating in quiet Sun regions, as well as of those originating in active regions, will continue to challenge space weather forecasters until reliable advance information can be obtained on the strength and direction of the magnetic fields of interplanetary CMEs [*Joselyn*, 1995].

[23] **Acknowledgments.** We thank Jeffrey Love for sharing his extended *Dst* index in advance of publication, Leif Svalgaard for assistance with the solar wind reconstruction, Pat McIntosh for providing Figure 2, and Dave Webb for comments on the manuscript. We thank both referees for helpful comments.

[24] Zuyin Pu thanks Joan Feynman and another reviewer for their assistance in evaluating this paper.

References

Allen, J., L. Frank, H. Sauer, and P. Reiff (1989), Effects of the March 1989 solar activity, *Eos Trans. AGU*, *70*(46), 1479, doi:10.1029/89EO00409.

Bruzek, A. (1952), On a type of flare associated with ascendant dark filaments, *Observatory*, *72*, 154.

Bruzek, A., and C. J. Durrant (Eds.) (1977), *Illustrated Glossary for Solar and Solar-Terrestrial Physics*, D. Reidel, Boston, Mass.

Cliver, E. W., and N. U. Crooker (1993), A seasonal dependence for the geoeffectiveness of eruptive solar events, *Sol. Phys.*, *145*, 347, doi:10.1007/BF00690661.

Cliver, E. W., and L. Svalgaard (2004), The 1859 solar-terrestrial disturbance and the current limits of extreme space weather activity, *Sol. Phys.*, *224*, 407, doi:10.1007/s11207-005-4980-z.

Cliver, E. W., J. Feynman, and H. B. Garrett (1990), An estimate of the maximum speed of the solar wind, *J. Geophys. Res.*, *95*, 17,103, doi:10.1029/JA095iA10p17103.

Crooker, N. U., and E. W. Cliver (1994), Postmodern view of M-regions, *J. Geophys. Res.*, *99*, 23,383, doi:10.1029/94JA02093.

Dodson, H. W., and E. R. Hedeman (1964), Problems of differentiation of flares with respect to geophysical effects, *Planet. Space Sci.*, *12*, 393, doi:10.1016/0032-0633(64)90034-0.

Feynman, J., and S. F. Martin (1995), The initiation of coronal mass ejections by newly emerging magnetic flux, *J. Geophys. Res.*, *100*, 3355, doi:10.1029/94JA02591.

Feynman, J., and A. Ruzmaikin (2004), A high-speed erupting-prominence CME: A bridge between types, *Sol. Phys.*, *219*, 301, doi:10.1023/B:SOLA.0000022996.53206.9d.

Fox, P., P. McIntosh, and P. R. Wilson (1998), Coronal holes and the polar field reversals, *Sol. Phys.*, *177*, 375, doi:10.1023/A:1004939014025.

Gopalswamy, N., A. Lara, S. Yashiro, M. L. Kaiser, and R. A. Howard (2001), Predicting the 1 AU arrival times of coronal mass ejections, *J. Geophys. Res.*, *106*, 29,207, doi:10.1029/2001JA000177.

Gopalswamy, N., S. Yashiro, G. Michalek, H. Xie, R. P. Lepping, and R. A. Howard (2005a), Solar source of the largest geomagnetic storm of cycle 23, *Geophys. Res. Lett.*, *32*, L12S09, doi:10.1029/2004GL021639.

Gopalswamy, N., S. Yashiro, Y. Liu, G. Michalek, A. Vourlidas, M. L. Kaiser, and R. A. Howard (2005b), Coronal mass ejections and other extreme characteristics of the 2003 October–November solar eruptions, *J. Geophys. Res.*, *110*, A09S15, doi:10.1029/2004JA010958.

Gosling, J. T. (1993), The solar flare myth, *J. Geophys. Res.*, *98*, 18,937, doi:10.1029/93JA01896.

Gosling, J. T., E. Hildner, R. M. MacQueen, R. H. Munro, A. I. Poland, and C. L. Ross (1976), The speeds of coronal mass ejection events, *Sol. Phys.*, *48*, 389, doi:10.1007/BF00152004.

Gulbrandsen, A. (1973), Relation between coronal λ 5303 intensity, recurrent geomagnetic storms, and solar sector structure, *J. Geophys. Res.*, *78*, 4787, doi:10.1029/JA078i022p04787.

Gurnett, D. A., W. S. Kurth, S. C. Allendorf, and R. L. Poynter (1993), Radio emission from the heliopause triggered by an interplanetary shock, *Science*, *262*, 199, doi:10.1126/science.262.5131.199.

Hale, G. E. (1931), The spectrohelioscope and its work, Part III: Solar eruptions and their apparent terrestrial effects, *Astrophys. J.*, *73*, 379, doi:10.1086/143316.

Hudson, H. S., and E. W. Cliver (2001), Observing coronal mass ejections without coronagraphs, *J. Geophys. Res.*, *106*, 25,199.

Jones, H. S. (1955), *Sunspot and Geomagnetic Storm Data Derived from Greenwich Observations, 1874–1954*, Her Majestys Stationery Off., London.

Joselyn, J. A. (1995), Geomagnetic activity forecasting: The state of the art, *Rev. Geophys.*, *33*, 383, doi:10.1029/95RG01304.

Joselyn, J. A., and P. S. McIntosh (1981), Disappearing solar filaments: A useful predictor of solar activity, *J. Geophys. Res.*, *86*, 4555, doi:10.1029/JA086iA06p04555.

Kahler, S. W. (1992), Solar flares and coronal mass ejections, *Annu. Rev. Astron. Astrophys.*, *30*, 113, doi:10.1146/annurev.aa.30.090192.000553.

Kappenman, J. G. (2006), Great geomagnetic storms and extreme impulsive geomagnetic field disturbance events An analysis of observational evidence including the great storm of May 1921, *Adv. Space Res.*, *38*(2), 188, doi:10.1016/j.asr.2005.08.055.

Kiepenheuer, K. O. (1964), An assembly of flare observations as related to theory, in *AAS-NASA Symposium on The Physics of Solar Flares*, p. 323, NASA, Washington, D. C.

Krieger, A. S., A. F. Timothy, and E. C. Roelof (1973), A coronal hole and its identification as the source of a high velocity solar wind stream, *Sol. Phys.*, *29*, 505, doi:10.1007/BF00150828.

Li, X., M. Temerin, B. T. Tsurutani, and S. Alex (2006), Modeling of 1–2 September 1859 super magnetic storm, *Adv. Space Res.*, *38*(2), 273, doi:10.1016/j.asr.2005.06.070.

Lockyer, N. (1909), The magnetic storm of September 25, 1909, and the associated solar disturbance, *Mon. Not. R. Astron. Soc.*, *70*, 12.

Love, J. J. (2007), A continuous long-term record of magnetic storm intensity and occurrence, *Eos Trans. AGU*, *88*(23), Jt. Assem. Suppl., Abstract SH54B-03.

Martin, S. F. (1998), Conditions for the formation and maintenance of filaments, *Sol. Phys.*, *182*, 107, doi:10.1023/A:1005026814076.

Mayaud, P. N. (1980), *Derivation, Use, and Meaning of Geomagnetic Indices*, *Geophys. Monograph Ser.*, vol. 22, AGU, Washington, D. C.

McAllister, A. H., M. Dryer, P. McIntosh, H. Singer, and L. Weiss (1996), A large polar crown coronal mass ejection and a "problem" geomagnetic storm: April 14–23, 1994, *J. Geophys. Res.*, *101*, 13,497, doi:10.1029/96JA00510.

McIntosh, P. S. (1979), *Annotated Atlas of H-Alpha Synoptic Charts for Solar Cycle 20 (1964–1974)*, *UAG-70*, NOAA, Boulder, Colo.

McIntosh, P. S. (1990), The classification of sunspot groups, *Sol. Phys.*, *125*, 251, doi:10.1007/BF00158405.

McIntosh, P. S. (1993), Coronal holes and solar predictions, in *Solar-Terrestrial Predictions–IV*, vol. 2, edited by J. Hruska et al., 20 pp., NOAA, Boulder, Colo.

McIntosh, P. S. (2003), Patterns and dynamics of solar magnetic fields and HeI coronal holes in cycle 23, in *Solar Variability as an Input to the Earth's Environment*, *Proc. ISCS 2003, Eur. Space Agency Spec. Publ.*, *ESA-SP 535*, 807.

Neupert, W. N., and V. Pizzo (1974), Solar coronal holes as sources of recurrent geomagnetic disturbances, *J. Geophys. Res.*, *79*, 3701, doi:10.1029/JA079i025p03701.

Newton, H. W. (1943), Solar flares and magnetic storms, *Mon. Not. R. Astron. Soc.*, *103*, 244.

Newton, H. W. (1944), Solar flares and magnetic storms (second paper), *Mon. Not. R. Astron. Soc.*, *104*, 4.

Newton, H. W. (1948), A distinctive geomagnetic epoch, 1941 June 9–14, *Observatory*, *68*, 60.

Richardson, I. G., et al. (2006), Major geomagnetic storms ($Dst \leq -100$ nT) generated by corotating interaction regions, *J. Geophys. Res.*, *111*, A07S09, doi:10.1029/2005JA011476.

Silverman, S. M. (1995), Low latitude auroras: The storm of 25 September 1909, *J. Atmos. Terr. Phys.*, *57*, 673, doi:10.1016/0021-9169(94)E0012-C.

Siscoe, G. L., N. U. Crooker, and L. Christopher (1978), A solar cycle variation of the interplanetary magnetic field, *Sol. Phys.*, *56*, 449, doi:10.1007/BF00152484.

Svalgaard, L. (1977), Geomagnetic activity: Dependence on solar wind parameters, in *Skylab Workshop Monograph on Coronal Holes*, edited by J. B. Zirker, chap. 9, p. 371, Columbia Univ. Press, New York.

Temerin, M., and X. Li (2002), A new model for the prediction of *Dst* on the basis of the solar wind, *J. Geophys. Res.*, *107*(A12), 1472, doi:10.1029/2001JA007532.

Watari, S., M. Kunitake, and T. Watanabe (2001), The Bastille Day (14 July 2000) event in historical large Sun-Earth connection events, *Sol. Phys.*, *204*, 425.

Webb, D. F. (1999), Final Report for NSF Award #9713460, Natl. Sci. Found., Arlington, Va.

Wright, C. S. (1991), Catalog of solar filament disappearances 1964–1980, *UAG-100*, World Data Cent. A for Sol.-Terr. Phys., Boulder, Colo.

Zhang, J., et al. (2007), Solar and interplanetary sources of major geomagnetic storms ($Dst \leq -100$ nT) during 1996–2005, *J. Geophys. Res.*, *112*, A10102, doi:10.1029/2007JA012321.

K. S. Balasubramaniam and E. W. Cliver, Space Vehicles Directorate, Air Force Research Laboratory, 29 Randolph Road, Hanscom Air Force Base, MA 01731-3010, USA. (afrl.rvb.pa@hanscom.af.mil)

X. Li, Laboratory for Atmospheric and Space Physics, 1234 Innovation Drive, Boulder, CO 80303-7814, USA.

N. V. Nitta, Lockheed Martin Solar and Astrophysics Laboratory, Department H1-12, Building 252, 3251 Hanover Street, Palo Alto, CA 94304, USA.